Genet. Res., Camb. (2006), **87**, *pp.* 45–60. © 2006 Cambridge University Press
doi:10.1017/S0016672306007944 Printed in the United Kingdom

Bayesian analyses of multiple epistatic QTL models for body weight and body composition in mice

NENGJUN YI[1,2], DENISE K. ZINNIEL[3], KYOUNGMI KIM[1], EUGENE J. EISEN[4], ALFRED BARTOLUCCI[1], DAVID B. ALLISON[1,2] AND DANIEL POMP[5]*
[1] *Department of Biostatistics, Section on Statistical Genetics, University of Alabama, Birmingham, AL 35294, USA*
[2] *Clinical Nutrition Research Center, University of Alabama, Birmingham, AL 35294, USA*
[3] *Department of Veterinary and Biomedical Sciences, University of Nebraska, Lincoln, NE 68583, USA*
[4] *Department of Animal Science, North Carolina State University, Raleigh, NC 27695, USA*
[5] *Departments of Nutrition, Cell and Molecular Physiology, University of North Carolina, Chapel Hill, NC 27599, USA*

(*Received 18 August 2005 and in revised form 29 November 2005*)

Summary

To comprehensively investigate the genetic architecture of growth and obesity, we performed Bayesian analyses of multiple epistatic quantitative trait locus (QTL) models for body weights at five ages (12 days, 3, 6, 9 and 12 weeks) and body composition traits (weights of two fat pads and five organs) in mice produced from a cross of the F1 between M16i (selected for rapid growth rate) and CAST/Ei (wild-derived strain of small and lean mice) back to M16i. Bayesian model selection revealed a temporally regulated network of multiple QTL for body weight, involving both strong main effects and epistatic effects. No QTL had strong support for both early and late growth, although overlapping combinations of main and epistatic effects were observed at adjacent ages. Most main effects and epistatic interactions had an opposite effect on early and late growth. The contribution of epistasis was more pronounced for body weights at older ages. Body composition traits were also influenced by an interacting network of multiple QTLs. Several main and epistatic effects were shared by the body composition and body weight traits, suggesting that pleiotropy plays an important role in growth and obesity.

1. Introduction

Obesity is a highly prevalent condition with adverse health effects and multifactorial aetiology. Though highly heritable, the genetic architecture of obesity is quite complex and remains to be fully elucidated (Allison *et al*., 2002; Dong *et al*., 2003; Pomp *et al*., 2004). Some genes involved in predisposition to obesity may only be detectable with models that accommodate epistasis. Indeed, some studies have shown that obesity and other diseases in both humans and rodents are influenced by epistasis (Brockmann *et al*., 2000, 2004; Allison *et al*., 2002; Yi *et al*., 2004*a*, *b*; Carlborg & Haley, 2004). These studies have shown that some QTLs may lack marginal effects but significantly affect the trait if they are evaluated jointly with other loci. Therefore, more explicit analysis of complex interactions among multiple genes is desired in discovering of genes underlying obesity and in better understanding how genetic predisposition is regulated.

We report here the detection of epistatic QTLs for growth and obesity in a backcross population derived from two diverse mouse populations: an inbred line (M16i) derived by brother–sister mating from a line that had undergone long-term selection for rapid post-weaning weight gain, and an inbred line (CAST/Ei) derived from wild mice. Using traditional interval mapping and multivariate techniques (Lander & Botstein, 1989; Haley & Knott, 1992), several genomic regions have been identified to harbour QTLs influencing principal components of organ weights and limb bone lengths in this backcross (Pomp, 1997; Leamy *et al*., 2002). However, other obesity-related traits that were measured in this population, such as body weights and fat pads, have not been investigated. Furthermore, statistical

* Corresponding author. Department of Nutrition, University of North Carolina, Chapel Hill, NC 27599, USA. Tel: +1 (919) 9660013. Fax: +1 (801) 3823686. e-mail: dpomp@unc.edu

methods for mapping multiple and epistatic QTLs were not previously employed to analyse these data. In this study, we used the Bayesian model selection method developed by Yi *et al.* (2005) to comprehensively investigate the genetic architecture of body weights, fat pad measurements and organ weights.

2. Materials and methods

(i) *Mouse lines and crosses*

Mice used in this study were from two distinct genetic backgrounds: the inbred high-growth selection line, M16i, and the inbred line of wild origin, *Mus musculus castaneus* (CAST/Ei; The Jackson Laboratory, Bar Harbor, ME). M16i originated from an ICR base and was derived from M16, which underwent long-term selection for rapid post-weaning (3–6 weeks) weight gain (Hanrahan *et al.*, 1973; Eisen, 1975). ICR stands for Institute for Cancer Research, an albino random-bred mouse line. The M16 line is characterized by increased growth rates and body weights and moderate obesity (Allan *et al.*, 2004). CAST/Ei (CAST), one of the four morphologically and biochemically distinct *Mus musculus* subspecies, exhibits small size and a lean body composition.

Development of the backcross population and details of animal husbandry have been described earlier (Leamy *et al.*, 2002). Briefly, CAST males were mated to M16i females, and seven F_1 males were backcrossed to M16i females, resulting in 54 litters with a total of 421 mice (213 males, 208 females) reaching adult age (12 weeks). All mice were reared in an environment of 21 °C, 55% relative humidity, and a 12 : 12 h light : dark cycle, following NIH guidelines for animal care. At birth (day 0), litters were standardized to a postnatal fraternity size of 10. Pups were weaned at day 21 and housed in groups of 2–4 per cage by sex. Mice were provided *ad libitum* access to water and feed (Purina Mouse Chow 5015 from mating until weaning and Purina Laboratory Chow 5001 from weaning and throughout phenotypic evaluation).

(ii) *Phenotypic traits and markers*

Body weights were recorded on all backcross mice at day 12 and at 3, 6, 9 and 12 weeks of age (12 d, 3 wk, 6 wk, 9 wk and 12 wk). Each mouse was killed at 12 wk of age, and a tail clip was frozen for later extraction of genomic DNA. Heart (HRT), liver (LIV), spleen (SPL), right kidney (KID), right epididymal (males) or perimetrial (females) fat pad (GON) and right hindlimb subcutaneous fat pad (SUB) were weighed (wet weights) in all mice. An additional trait analysed was FAT, the sum of GON and SUB. The right testis (TES) was weighed in male mice.

Ninety-two fully informative microsatellite markers spanning the 19 autosomes were genotyped in the backcross sample (Leamy *et al.*, 2002) (Table 1). Genotypes were determined by standard PCR and agarose gel electrophoresis protocols. The mating design used in this study did not enable screening of the sex chromosomes. Marker linkage maps were generated with MAPMAKER/EXP (Lincoln *et al.*, 1992) as described by Leamy *et al.* (2002).

(iii) *Statistical analyses*

Prior to QTL analyses, phenotypic data were adjusted by obtaining residuals from a general linear model including environmental effects attributed to sex, litter size, sire and family. Residuals were used as new phenotypes in the QTL analysis. To search for QTLs across the entire genome, we partitioned each chromosome with a 1 cM grid, resulting in 1214 ($=H$) possible loci across the genome, and assumed that the possible QTLs occur at these fixed loci. The problem of inferring the number and locations of multiple QTLs is equivalent to the problem of selecting a subset of 1214 possible loci that fully explains the genetically determined proportion of the phenotypic variation. Although any complex trait may be influenced by many QTLs, the number of detectable QTLs is much smaller than H. Using the Bayesian model selection framework of Yi *et al.* (2005), we placed a constraint on the upper bound of detectable QTLs (L) and restricted attention to models with fewer than L QTLs. The phenotypic values can be expressed as

$$y_i = \mu + \sum_{q=1}^{L} \gamma_q x_{iq} a_q + \sum_{q_1 < q_2}^{L} \gamma_{q_1 q_2} x_{iq_1} x_{iq_2} b_{q_1 q_2} + e_i,$$
$$i = 1, 2, \cdots, n,$$

where n is the number of mice; y_i is the phenotypic value of the ith mouse; μ is the overall mean; x_{iq} is the indicator variable denoting the genotype of putative QTL q for mouse i and is defined by 0·5 or −0·5 for the two genotypes, CM and MM, where C and M represent the CAST and M16i alleles, respectively; a_q represents the main effect of putative QTL q; $b_{q_1 q_2}$ is the epistatic effect between QTLs q_1 and q_2; γ_q is a binary indicator variable for the main effect of putative QTL q, taking value 1 if QTL q has a main effect and 0 otherwise, and $\gamma_{q_1 q_2}$ is a binary indicator variable for the epistatic effect between QTLs q_1 and q_2, taking value 1 if QTLs q_1 and q_2 interact and 0 otherwise; and e_i is the residual error assumed to follow $N(0, \sigma^2)$, where σ^2 is the residual variance. Note that the introduction of the effect indicators facilitates setting up Markov chain Monte Carlo (MCMC) algorithms (Yi *et al.*, 2005).

In the above model, the main effect, a_q, quantifies the difference between genotypic values of CM and

https://doi.org/10.1017/S0016672306007944 Published online by Cambridge University Press

Table 1. *Microsatellite markers genotyped and their chromosomal locations in Haldane units (cM)*[a]

Chromosome	Marker	cM	Chromosome	Marker	cM
1	D1MIT4	12	10	D10MIT16	16
	D1MIT9	45		D10MIT31	29
	D1MIT140	55		IGF-1	41
	D1MIT17	97		D10MIT13	57
2	D2MIT1	1	11	D11MIT63	2
	D2MIT79	13		D11MIT5	37
	D2MIT120	15		D11MIT11	67
	D2MIT157	30	12	D12NDS11	6
	D2MIT61	34		D12MIT5	41
	D2MIT37	43		D12MIT20	75
	D2NDS1	53	13	D13MIT15	10
	D2MIT103	58		D13MIT181	16
	D2MIT133	60		D13MIT311	20
	D2MIT164	63		D13MIT314	29
	D2MIT224	65		D13MIT169	31
	D2MIT166	70		D13MIT36	37
	D2MIT22	73		D13MIT51	41
	Agouti	75		D13MIT53	50
	GHRH	76		D13MIT263	52
	D2MIT49	80	14	D14MIT10	3
	D2MIT25	90		D14MIT32	30
	D2MIT147	93		D14MIT42	48
	D2MIT174	101	15	D15MIT11	10
	D2MIT200	105		D15MIT131	12
3	D3MIT46	14		D15MIT86	19
	D3MIT10	35		D15MIT121	23
	D3MIT31	75		D15MIT3	30
4	D4MIT39	11		D15MIT64	35
	D4MIT27	36		D15MIT29	39
	D4MIT33	78		D15MIT107	44
5	D5MIT48	1		PPAR	48
	D5MIT24	60		D15MIT34	62
	D5MIT51	92	16	D16MIT29	13
6	D6MIT50	3		D16MIT14	33
	D6NDS5	36		D16MIT7	45
	D6MIT14	70	17	D17MIT22	19
7	D7MIT55	15		D17MIT7	33
	D7MIT37	57		D1739	45
	D7MIT46	97	18	D18MIT19	2
8	D8MIT4	14		D18MIT10	17
	D8MIT25	21		D18MIT51	27
	D8MIT75	26		D18NDS1	73
	D8MIT42	110	19	D19MIT29	4
9	D9MIT2	17		D19MIT11	38
	D9MIT10	43		D19MIT1	52
	D9MIT18	75		D19MIT6	64

[a] The location of the first marker on each chromosome was taken from the Mouse Genome Database.

MM. Therefore, a positive (negative) main effect implies that the CAST allele promotes (reduces) the phenotype. Similarly, a positive (negative) epistasis promotes (reduces) the phenotypes of mice with double homozygotes (MM/MM) and double heterozygotes (CM/CM) at the corresponding two loci. Additionally, QTL analyses for all the fat pads and the organ weights were performed including 12 wk as a covariate in the above model. This adjustment can remove any linear influence of body weight on the fat pads and the organ weights and thus attempts to identify alternate sets of QTLs involved in different pathways responsible for the fluctuating patterns of phenotypic and genetic correlations observed among the various traits.

Based on the above multiple epistatic QTL model, we used the Bayesian model selection method developed by Yi *et al*. (2005) to jointly infer the number, positions, main and epistatic effects of multiple QTLs. Our approach proceeded by setting up a likelihood

https://doi.org/10.1017/S0016672306007944 Published online by Cambridge University Press

function for the phenotype based on the above model and assigning prior distributions to all unknowns in the model. These induced a posterior distribution on the unknown quantities that contains all the available information for inference of the genetic architecture of the trait. We first analysed the data using the interval mapping method based on a single-QTL model (Lander & Botstein, 1989), and then used the number of significant QTLs detected in the interval mapping to choose an upper bound of detectable QTLs and specify prior distributions for the indicator variables of main and epistatic effects. A LOD score of 3·3 was used to assess statistical significance at the 5% genome-wide level (Lander & Kruglyak, 1995). This threshold value approximately equalled those obtained by permutation tests (Leamy *et al*., 2002). The upper bound of detectable QTLs was then set to be $L = l_m + 2 + 3\sqrt{l_m + 2}$, where l_m is the number of main-effect QTLs detected in the interval mapping. The prior probabilities for the indicators of main effects and epistatic interactions were chosen to be l_m/L and $1 - \left[\frac{1-(l_m+2)/L}{1-l_m/L}\right]^{1/L-1}$, respectively (Yi *et al*., 2005). The positions of QTLs were independent and uniformly distributed over the H possible loci. We used non-informative distributions for μ and σ^2. The prior for each genetic effect was chosen to be the hierarchical mixture prior $N(0, \gamma\sigma^2(\mathbf{x}^T\mathbf{x})^{-1})$, where γ and $\mathbf{x}$ are the effect indicator and the vector of the coefficients for the corresponding effect, respectively.

The MCMC algorithm developed by Yi *et al*. (2005) was employed to generate posterior samples from the joint posterior distribution of all unknowns, by updating each parameter from its conditional posterior distribution in each of iterations. The MCMC algorithms were started with no QTL in the model. In each analysis, the MCMC sampler was run for 4×10^5 cycles after discarding the first 2000 cycles for the burn-in period. The chain was thinned (one iteration in every 20 cycles was saved) to reduce serial correlation in the stored samples, so that the total number of samples kept in the posterior analysis was 2×10^4. The stored samples (posterior samples) were used to infer the genetic architecture of the trait analysed. Convergence diagnostics assessed by the R package CODA (Plummer *et al*., 2005) showed that our algorithm performed well.

Each locus may affect the trait through its main effects and/or interactions with other loci (epistasis). Therefore, the larger the main effect and/or epistatic effects of a locus, the more frequently the locus is included in the model. This can be measured by the posterior inclusion probability of each possible locus ζ_h ($h = 1, 2, \ldots, H$), $p(\zeta_h|\mathbf{y})$, estimated as the frequency with which the locus ζ_h appeared in the posterior samples, where $\mathbf{y}$ is the vector of phenotypic values. The most likely position of QTLs in a certain region was estimated as the locus that produces the highest posterior inclusion probability. From $p(\zeta_h|\mathbf{y})$, we obtained the cumulative distribution function per chromosome, defined as $F_c(x|\mathbf{y}) = \sum_{\zeta_h=0}^{x} p(\zeta_h|\mathbf{y})$ for any position x on chromosome c. The fact that the cumulative distribution function at the last position is greater than 1 provides evidence of multiple QTLs at the corresponding chromosome. The posterior inclusion probability of an epistatic effect between two loci was estimated as the frequency which the epistasis appeared in the posterior samples. We reported all epistatic effects with the cumulative posterior inclusion probabilities for the corresponding chromosomes greater than 10%. The Bayes factors of these interactions, defined as the ratio of posterior and prior probabilities, are fairly high (>20) (Yi *et al*., 2005). The main effect and the proportion of phenotypic variance explained by the main effect at any locus were calculated using the posterior samples containing the locus. Similarly, we estimated the epistatic effect and the proportion of phenotypic variance explained by the epistasis.

3. Results

(i) *Body weights*

Interval mapping detected significant chromosomal intervals for all age-specific body weights: chromosomes 4 and 18 for 12 d, chromosomes 1 and 18 for 3 wk, chromosomes 1 and 2 for 6 wk, chromosomes 2 and 15 for 9 wk, and chromosomes 2, 11 and 15 for 12 wk (Table 2). There were additional suggestive QTLs detected for body weight at each age, with LOD scores close to the threshold used (not shown here). Some chromosomes (e.g. 2 and 15) showed two peaks.

There was strong evidence for age-dependent genetic regulation, with no single main-effect QTL being present at all ages. A QTL present in proximal chromosome 4 affecting weight at the preweaning age of 12 d was not present at older ages. Two other QTLs with strong main effects on body weights of mice at weaning (3 wk), but not on older mice, were located in the central regions of chromosomes 1 and 18, respectively. Conversely, a significant and strong QTL located in the central region of chromosome 2 for body weights of older mice (6 wk, 9 wk and 12 wk) was not evident for body weights of younger mice. In addition, chromosomes 11 and 15 also harboured QTLs affecting body weight of older mice only.

Profiles of posterior inclusion probabilities for each locus across the genome and cumulative posterior probabilities for each chromosome are depicted in the top panel of Fig. 1. The main effects of QTLs detected in the interval mapping were also detected in the Bayesian analysis of the epistatic model. Peaks of the profiles of posterior inclusion probability overlapped

https://doi.org/10.1017/S0016672306007944 Published online by Cambridge University Press

Table 2. *Interval mapping of body weight: locations (cM), LOD scores and confidence intervals (CI) of QTLs*

Trait[a]	Chromosome	Location	LOD[b]	CI[c]
12 d	4	17	3·41	11–41
	18	22	3·34	6–72
	18	48	4·27	19–65
3 wk	1	72	5·74	57–86
	18	45	4·71	13–60
6 wk	1	68	7·26	52–81
	2	43	3·40	36–64
	2	60	3·34	36–64
9 wk	2	62	13·65	54–66
	2	78	10·63	72–85
	15	42	3·54	32–62
	15	58	3·36	32–62
12 wk	2	66	16·20	59–68
	2	77	15·21	74–83
	11	23	4·14	7–52
	15	43	4·16	34–62
	15	56	3·93	34–62

[a] Body weights at day 12 and at 3, 6, 9 and 12 weeks of age (12 d, 3 wk, 6 wk, 9 wk and 12 wk).
[b] The LOD 3·3 criterion is used for significance.
[c] cM location where the LOD score is one less than the peak.

those of LOD scores. The epistatic analyses found further age-specific QTLs. For example, the non-epistatic analysis failed to detect QTLs on chromosomes 1 and 18 affecting body weights of older mice, but the presence of such QTLs was found in the epistatic model with a high posterior inclusion probability (~70%) for 9 wk and 12 wk. The posterior modes of these two epistatic QTLs were close to the markers D1MIT140 and D18NDS1, respectively, for both 9 wk and 12 wk. Although the main effects of these QTLs were relatively weak, they affected body weights of older mice mainly through epistatic interactions. The epistatic interaction between chromosomes 1 and 18 was included in the epistatic model with probability of ~60% and ~50%, respectively, for 9 wk and 12 wk (Table 3). However, this interaction did not affect body weights of younger mice.

The number of epistatic interactions varied temporally. Variations of body weight at older ages (6 wk, 9 wk and 12 wk) included more epistatic effects than at younger ages (12 d and 3 wk). For all ages, there were a total of eight chromosomes involved in interactions. The most active was chromosome 1, which interacted with four other chromosomes for body weights at different ages. Other frequently involved chromosomes included 2, 13 and 18. Three two-way interactions (chromosomes 1 and 18, 1 and 4, and 2 and 13) were observed at both 9 wk and 12 wk. However, other detected epistatic interactions affected body weight at only one time point.

Detected QTLs showed a complex pattern of genetic effects on body weight. Profiles of the location-wise main effects and the proportion of phenotypic variance explained by the main effects are displayed in the bottom panel of Fig. 1. Almost all loci across the genome showed positive main effects on body weights of younger mice but negative main effects on body weights of older mice. This finding implies that inheriting a CAST allele at any locus increased body weights at younger ages but reduced body weights of older mice. The main effects of the strongest QTL on chromosome 2 accounted for ~15% of the phenotypic variances at 9 wk and 12 wk. The proportions of the phenotypic variances contributed by the main effects of other detected QTLs ranged from 1 to 11%.

Estimates of epistatic effects and proportions of phenotypic variances explained by these epistatic interactions (Table 3) demonstrate that each interaction explained a low (but detectable) percentage of the phenotypic variance, ranging from 1·3% to 4·1%. A positive (negative) epistasis promotes (reduces) the phenotypes of mice that are double homozygotes (M16i/M16i and M16i/M16i) and double heterozygotes (M16i/CAST and M16i/CAST) at the corresponding two loci. All interactions detected at younger ages (12 d, 3 wk and 6 wk) were estimated to be negative. For body weights of older mice (9 wk and 12 wk), both positive and negative epistatic effects were observed. For example, the interaction of chromosomes 1 and 18 was positive for 9 wk and 12 wk, while the interaction of chromosomes 2 and 13 was negative for body weights at 6 wk, 9 wk and 12 wk.

(ii) *Fat pad weights*

Maximum likelihood (ML) interval mapping detected significant QTLs for individual fat pad weights (GON and SUB) and the composite trait FAT on chromosomes 2, 13 and 15 (Table 4). The strongest QTL was identified on chromosome 2 at 77 cM with LOD scores ranging from 17 to 20 for the three fatness traits. This QTL also had the largest main effect on body weights at 9 wk and 12 wk. As observed for body weight, chromosome 15 showed multiple peaks; the highest peak (LOD of ~5) is observed at 35 cM, while additional sub-peaks are seen above the significance threshold in the interval 14–25 cM. Chromosome 13 was detected to influence the fatness traits. This fat-specific region did not influence body weights or weights of the organs measured in this study.

As shown in the profiles of posterior inclusion probability and cumulative function, QTLs on chromosomes 2, 13 and 15 were also detected in the

https://doi.org/10.1017/S0016672306007944 Published online by Cambridge University Press

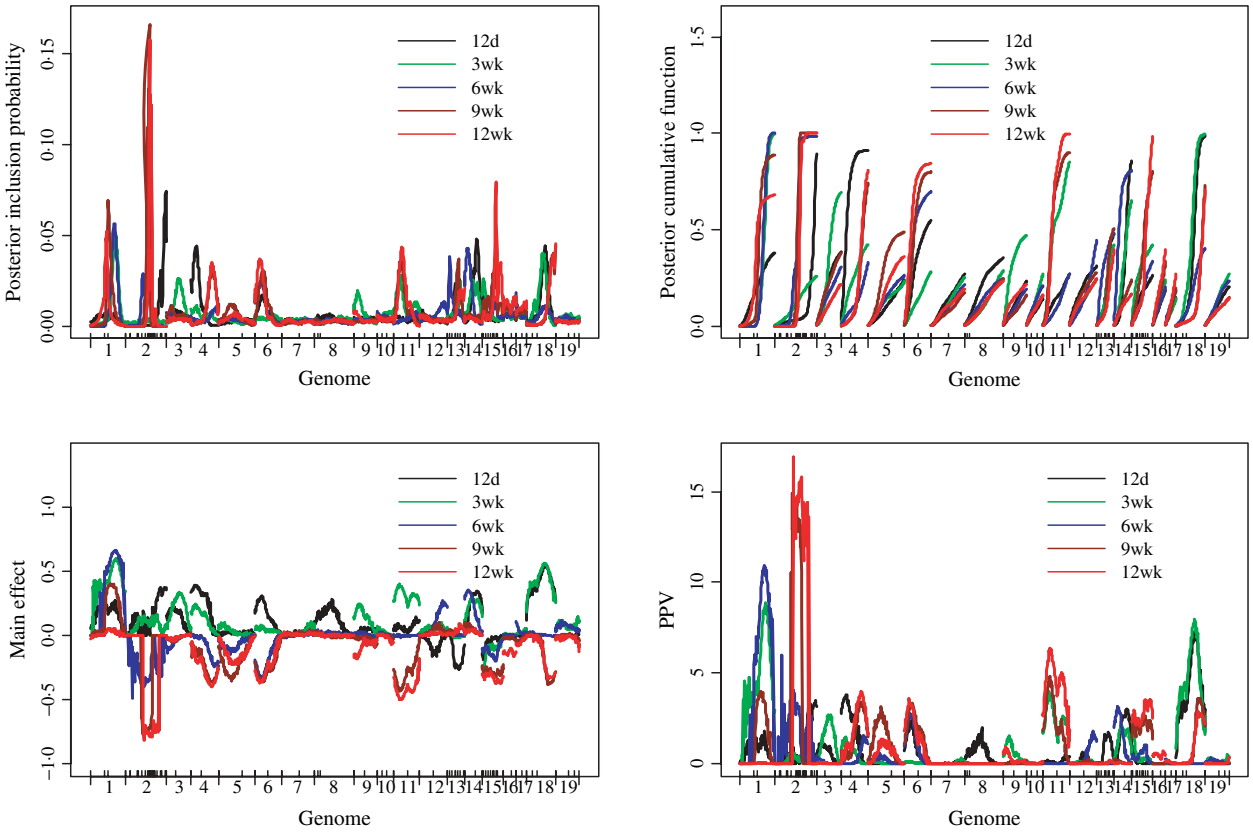

Fig. 1. Genome-wide epistatic analysis of body weights: profiles of posterior inclusion probability, cumulative probability function, posterior means of main effect and proportion of phenotypic variance explained by main effect (PPV %). On the *x*-axis, outer tick marks represent chromosomes and inner tick marks represent markers. 12 d, 3 wk, 6 wk, 9 wk and 12 wk represent body weights at day 12 and at 3, 6, 9 and 12 weeks of age, respectively.

Bayesian analysis of the epistatic model (Fig. 2). Peaks of the profiles of posterior inclusion probability overlapped those of LOD scores. Similarly to body weights at older ages, the QTLs on chromosomes 2 and 15 had negative main effects. However, the fat-specific QTL on chromosome 13 had positive effects, indicating that the presence of a CAST allele increased fat. The three main-effect QTLs on chromosomes 2, 13 and 15 were estimated to explain ∼18%, 4% and 3% of the phenotypic variances, respectively.

Analyses of epistasis found strong evidence for QTLs on chromosomes 1, 18 and 19 with high cumulative probabilities (close to 1) for all three fat depot traits, unadjusted for body weight, and suggestive evidence of QTLs on chromosomes 6, 7, 11 and 14. The QTLs on chromosomes 1, 18 and 19 were estimated to have weak main effects and thus were detected in the epistatic model mainly due to epistatic interactions. The posterior modes of these three epistatic QTLs were close to the markers D1MIT140, D18NDS1 and D19MIT11, respectively, for all three fat pads. Table 5 shows epistatic interactions between chromosomes with >10% of posterior inclusion probability. There were a total of 10 chromosomal regions involved in interactions, including the regions with strong main effects on chromosomes 2, 13 and 15 as well as several other regions with weak main effects. As for body weights, interactions among the chromosomal regions with strong main effects (chromosomes 2, 13 and 15) were negative and, conversely, all other interactions involving at least one region with weak main effect were positive.

The strongest interaction for fat occurred between QTLs on chromosomes 1 and 18, which also strongly influenced the phenotypic variation of body weights at 9 wk and 12 wk. This interaction was included in the epistatic model with high probabilities and explained ∼5% of the phenotypic variances for all three fat phenotypes. A region of chromosome 19 was found to interact with chromosomes 15 and 7. The interaction between the regions of chromosomes 19 and 15 was included in the model with ∼50% and 65% of probability, and explained ∼2% and 3% of the phenotypic variances for FAT and GON, respectively. Two interactions involving two main-effect QTLs, chromosomes 2 and 13 and chromosomes 13 and 15, were found to influence the fat traits. The first was included in the epistatic model with ∼96% and 55% of probabilities and explained

https://doi.org/10.1017/S0016672306007944 Published online by Cambridge University Press

Table 3. *Epistatic analysis of body weights: cumulative posterior inclusion probability, posterior mean of epistatic effect and proportion of phenotypic variance explained by the epistasis (PPV%)*

Trait[a]	Chromosome pair	Posterior probability	Epistasis	PPV
12 d	2 × 14	0·244	−0·499	1·8
3 wk	3 × 13	0·252	−0·619	2·7
6 wk	1 × 2	0·471	−0·627	2·8
	2 × 13	0·145	−0·435	1·3
	13 × 18	0·252	−0·718	3·5
9 wk	1 × 4	0·121	0·467	1·6
	1 × 11	0·424	0·598	2·3
	1 × 18	0·631	0·817	4·1
	2 × 13	0·402	−0·573	2·2
12 wk	1 × 4	0·434	0·680	3·1
	1 × 18	0·530	0·722	3·4
	2 × 13	0·210	−0·485	1·6
	13 × 15	0·107	−0·410	1·2

[a] Body weights at day 12 and at 3, 6, 9 and 12 weeks of age (12 d, 3 wk, 6 wk, 9 wk and 12 wk).

∼3% and 2% of the phenotypic variances for GON and FAT, respectively. The latter appeared to affect all three traits and explained ∼2% of the phenotypic variances.

As seen in the bottom panels of Table 4 and Fig. 3, the inclusion of 12 wk as a covariate in the analyses influenced detection of QTLs for fat depots. When removing variation due to 12 wk from the fat traits, both interval and Bayesian mapping revealed activity of QTLs on chromosomes 5, 14 and 17, where there had been no QTL detected previously for the unadjusted traits. These fat-specific main effects were positive on chromosomes 5 and 17 and negative on chromosome 14, and explained 3–6% of the phenotypic variances. When adjusted by 12 wk, the QTL on chromosome 2 still influenced fat traits, indicating that this QTL probably has pleiotropic effects on body weight and fatness. Conversely, the main effect on chromosome 15 was eliminated after adjustment for body weight, suggesting that this locus had increased fat pad weights simply in proportion to increases in overall weight. Most of the strong epistatic interactions detected for unadjusted fat traits, such as chromosomes 1 and 18, 2 and 13, and 15 and 19, were still found to influence fatness after adjustment for body weight (Table 5). The posterior modes of these epistatic QTLs and the sign of these pleiotropic interactions remained unchanged.

(iii) *Organ weights*

Interval mapping for organ weights identified significant main-effect QTLs influencing LIV on chromosomes 2 and 11, SPL on chromosomes 4 and 9, and KID on chromosomes 1 and 18 (Table 6). Inclusion of 12 wk as a covariate in the model did not influence the results for HRT and TES, but greatly influenced the detection of QTLs for LIV, SPL and KID. The significant QTLs on chromosomes 2 and 11 for LIV were removed and lessened, respectively, when adjusted by 12 wk. However, new QTLs were found for KID on chromosomes 2 and 3 and for SPL on chromosomes 2 and 10 (Table 6).

Bayesian analysis of the multiple epistatic model identified all main-effect QTLs detected by interval mapping for both the unadjusted and the adjusted traits (Figs. 4 and 5). Peaks on the profiles of the posterior inclusion probability overlapped those of the LOD curves. As seen for body weights and fat traits, however, the curves of the posterior inclusion probability were much sharper than the LOD curve and thus provided more precise estimation of QTL locations. For both unadjusted and adjusted KID, for example, LOD score curves on chromosome 1 significantly spanned the whole chromosome, but curves of the posterior inclusion probability concentrated on a narrow region near D1MIT140 with high posterior cumulative probabilities. For unadjusted LIV and adjusted KID, there were three peaks on the profiles of the posterior inclusion probability on chromosome 2, and the posterior cumulative probabilities were 1·4, indicating the possibility of multiple QTLs.

The posterior mean profiles of location-wise main effects and variances explained by the main effects are displayed in Figs. 4 and 5. For LIV and SPL, main effects in all significant regions were negative, similar to the patterns for body weights at older ages and fat traits. Conversely, main effects in most chromosomal regions for HRT and TES were positive, indicating that a CAST allele promotes HRT and TES but reduces LIV and SPL. For KID, some chromosomes (e.g. 1, 2 and 3) showed positive effects and others (e.g. 18) negative effects. Main effects explained ∼5% to 17% of the phenotypic variances.

Organ weights are influenced by epistatic interactions (Table 7). The strongest interaction occurred between chromosomes 1 and 18 for KID, which also greatly influenced the variations of body weights at older ages and fat traits. This interaction was included in the models with 99% and 30% of posterior probability and explained ∼5% and 2% of the phenotypic variances for unadjusted and adjusted KID, respectively.

4. Discussion

(i) *Bayesian epistatic QTL mapping*

The introduction of genome-wide screening to detect QTLs affecting complex traits has recently drawn renewed interest to the importance of epistasis in the evolution and aetiology of disease-associated traits

https://doi.org/10.1017/S0016672306007944 Published online by Cambridge University Press

Table 4. *Interval mapping of fat traits: locations (cM), LOD scores and confidence intervals (CI) of QTLs*

		Location		LOD[b]		CI[c]	
Trait[a]	Chromosome	Unadjusted[d]	Adjusted[e]	Unadjusted	Adjusted	Unadjusted	Adjusted
FAT	2	77	81	20·60	6·83	72–83	70–90
	13	40	30	4·60	3·65	27–47	21–47
	15	35		4·54		31–42	
	15	24		3·63		12–28	
	5		31		3·56		6–61
GON	2	77	77	17·02	4·94	72–83	70–88
	13	41	29	4·59	3·47	27–47	22–47
	15	35		4·48		31–43	
	15	25		3·62		20–30	
	17		22		3·32		19–37
SUB	2	78	84	18·87	5·61	72–86	71–101
	13	34		3·56		26–47	
	15	35		3·49		10–43	
		14		3·41		10–43	
	14		30		3·70		16–43

[a] GON, SUB and FAT represent perimetrial fat pad, right hindlimb subcutaneous fat pad and the sum of the two fat pads, respectively.
[b] The LOD 3·3 criterion is used for significance.
[c] cM location where the LOD score is one less than the peak.
[d] No adjustment for body weight at 12 weeks of age.
[e] Adjustment for body weight at 12 weeks of age.

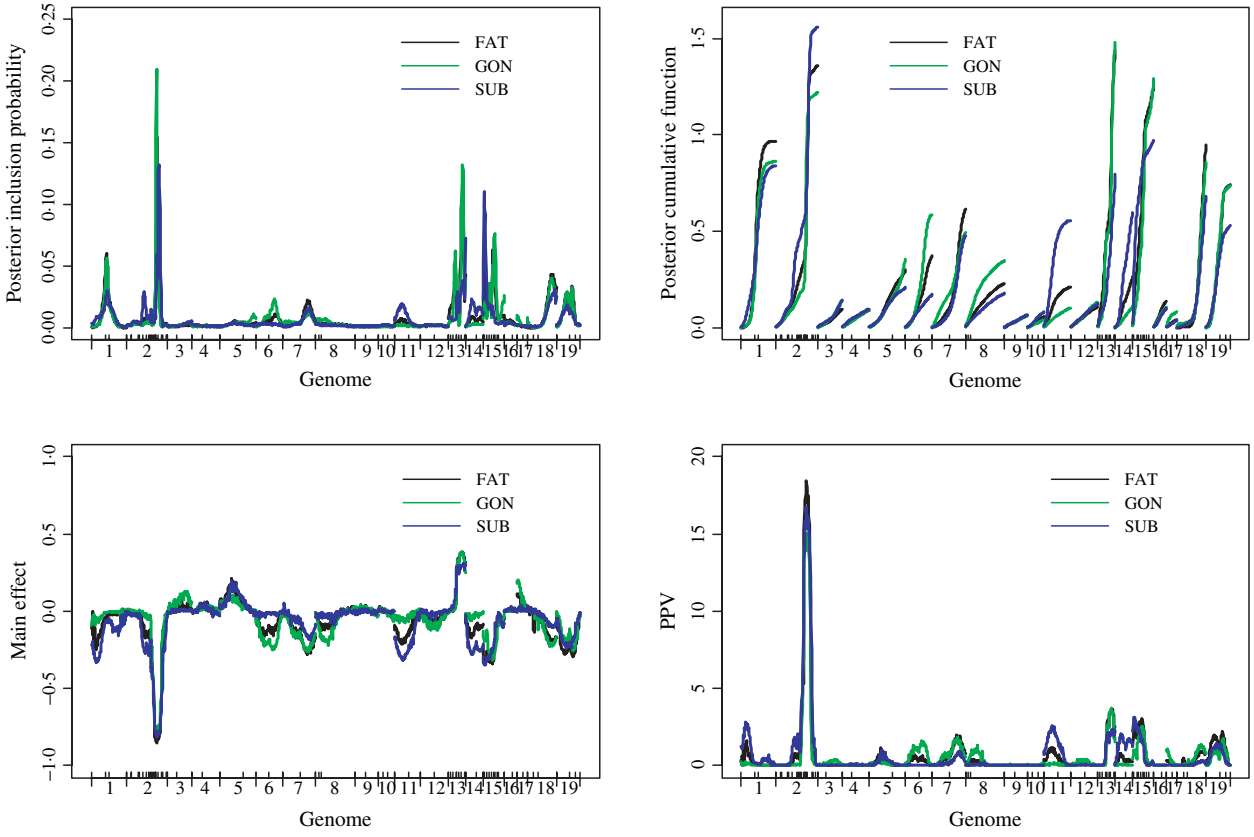

Fig. 2. Genome-wide epistatic analysis of fat traits under model without adjustment for body weight at 12 weeks: profiles of posterior inclusion probability, cumulative probability function, posterior means of main effect and proportion of phenotypic variance explained by main effect (PPV %). On the *x*-axis, outer tick marks represent chromosomes and inner tick marks represent markers. GON, SUB and FAT represent perimetrial fat pad, right hindlimb subcutaneous fat pad and the sum of the two fat pads, respectively.

https://doi.org/10.1017/S0016672306007944 Published online by Cambridge University Press

Table 5. *Epistatic analysis of fat traits: cumulative posterior inclusion probability, posterior mean of epistatic effect and proportion of phenotypic variance explained by the epistasis (PPV%)*

Trait[a]	Chromosome pair	Posterior probability		Epistasis		PPV	
		Unadjusted[b]	Adjusted[c]	Unadjusted	Adjusted	Unadjusted	Adjusted
FAT	1 × 18	0·942	0·719	0·931	0·722	5·4	3·2
	2 × 13	0·543	0·158	−0·541	−0·388	1·8	0·9
	2 × 14	0·155	0·125	0·523	0·420	1·7	1·1
	5 × 13	0·122	0·118	0·541	0·535	1·8	1·7
	7 × 19	0·231	0·114	0·618	0·471	2·3	1·3
	13 × 15	0·476	0·105	−0·557	−0·393	1·9	1·0
	15 × 19	0·452	0·423	0·579	0·563	2·1	1·9
	6 × 13	0·158		−0·568		2·0	
	2 × 5		0·424		−0·604		2·2
	2 × 7		0·179		0·479		1·4
GON	1 × 18	0·814	0·271	0·886	0·663	4·9	2·7
	2 × 13	0·959	0·591	−0·687	−0·543	2·9	1·8
	13 × 15	0·465	0·168	−0·588	−0·454	2·1	1·2
	15 × 19	0·641	0·745	0·659	0·674	2·7	2·8
	5 × 13	0·112		0·534		1·8	
	5 × 15	0·159		−0·651		2·6	
	6 × 8	0·120		0·666		2·7	
	6 × 13	0·219		−0·583		2·1	
	6 × 15	0·119		0·480		1·4	
	1 × 7		0·125		−0·529		1·7
SUB	1 × 18	0·630	0·324	0·839	0·658	4·3	2·7
	2 × 14	0·288	0·162	0·575	0·415	2·0	1·1
	7 × 19	0·275		0·686		2·9	
	13 × 15	0·102	0·332	−0·438	−0·704	1·1	3·0
	1 × 5						
	2 × 3		0·251		−0·609		2·3
	2 × 5		0·456		−0·688		2·9
	2 × 7		0·137		0·498		1·5

[a] GON, SUB and FAT represent perimetrial fat pad, right hindlimb subcutaneous fat pad and the sum of the two fat pads, respectively.
[b] No adjustment for body weight at 12 weeks of age.
[c] Adjustment for body weight at 12 weeks of age.

such as obesity and type 2 diabetes (Warden *et al*., 2004; Carlborg & Haley, 2004; Chesler *et al*., 2005; Moore, 2005; Segrè *et al*., 2005). This interest has fuelled research into statistical models traditionally used to interpret epistasis (Yang, 2004; Zeng *et al*., 2005) and has led to refined methods of estimating epistasis in QTL analyses (Carlborg *et al*., 2000; Yi & Xu, 2002; Yi *et al*., 2003, 2005; Zhang & Xu, 2005).

We adopted a Bayesian model selection method (Yi *et al*., 2005) to search for epistatic QTLs across the entire genome with effects on body weight, obesity and organ weights. Our Bayesian method used multiple QTL models and jointly inferred the number of QTLs, their genomic positions, and their main and epistatic effects simultaneously. Therefore, this Bayesian mapping method could detect multiple QTLs with any combination of main and pairwise epistatic effects in an interactive fashion. The Bayesian framework incorporates our prior information into analysis, and provides a robust inference of genetic architecture that incorporates model uncertainty by averaging over all possible models (Yi *et al*., 2005).

Our present Bayesian method separately analyses each of multiple traits. However, the phenotypes investigated in this study present significant correlations (not shown here), showing that joint analysis of these phenotypes may improve power for detecting QTLs. In particular, body weights at five ages describe growth and should be better treated as a function-valued trait (Wu *et al*., 2005). Joint analysis of multiple phenotypes can provide formal procedures to investigate the genetic mechanisms such as pleiotropy and close linkage (Jiang & Zeng, 1995; Wu *et al*., 2005). Extension of our Bayesian method to multiple traits will be pursued.

(ii) *Body weight QTLs*

At least three subsets of QTLs influencing growth in mice were found, including those that act early in life, those that act later in life, and those with effects

https://doi.org/10.1017/S0016672306007944 Published online by Cambridge University Press

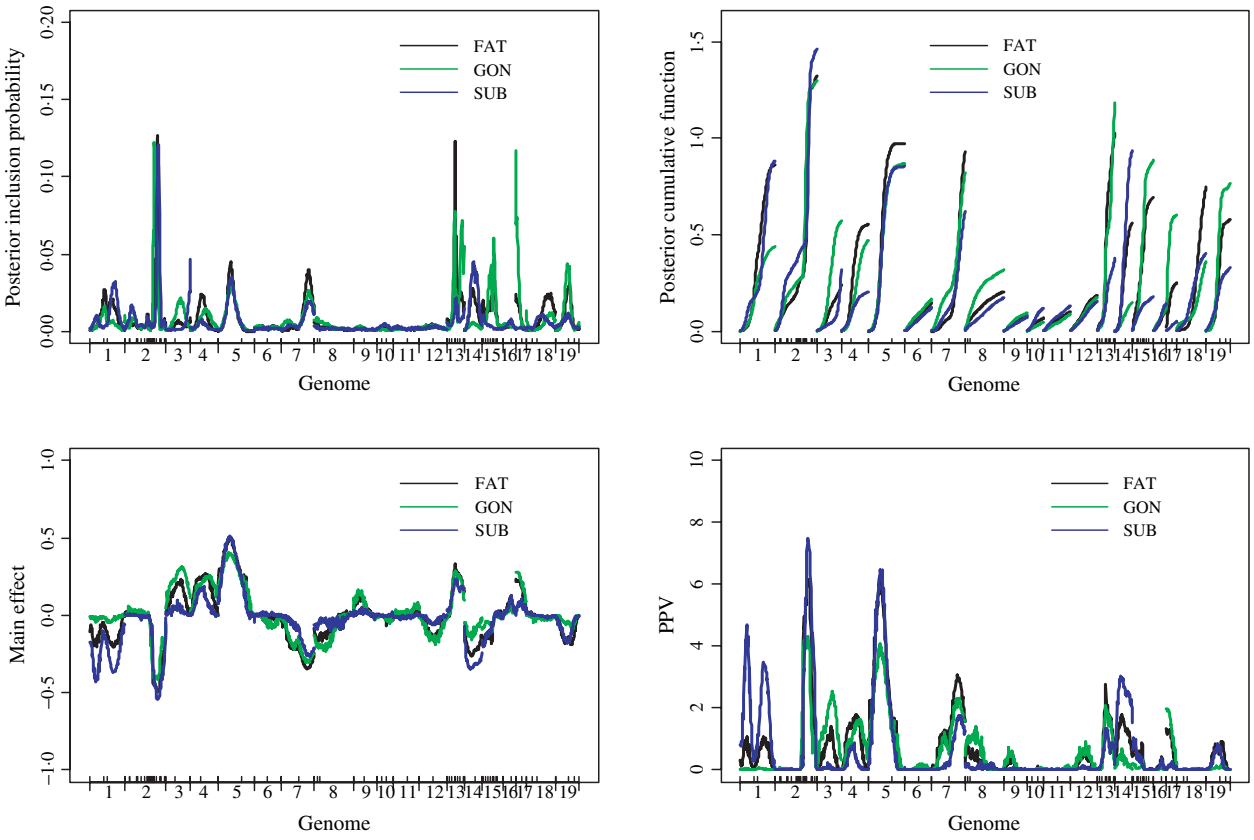

Fig. 3. Genome-wide epistatic analysis of fat traits under model including adjustment for body weight at 12 weeks: profiles of posterior inclusion probability, cumulative probability function, posterior means of main effect and proportion of phenotypic variance explained by main effect (PPV %). On the *x*-axis, outer tick marks represent chromosomes and inner tick marks represent markers. GON, SUB and FAT represent perimetrial fat pad, right hindlimb subcutaneous fat pad and the sum of the two fat pads, respectively.

throughout ontogeny. Such findings confirm previous reports (Cheverud *et al.*, 1996; Vaughn *et al.*, 1999; Morris *et al.*, 1999; Rocha *et al.*, 2004*a*; Brockmann *et al.*, 2004). The presence of such subsets of genes is not surprising given the low phenotypic and genetic correlations that were found between early and late body weights or growth rates in these data (Leamy *et al.*, 2002) and other studies (Rutledge *et al.*, 1972; Atchley *et al.*, 1984; Cheverud *et al.*, 1996). Atchley *et al.* (1997) provided further evidence for independent genes affecting early and late growth by successfully using selection indexes to modify early growth while constraining changes in growth at a later age. Furthermore, it is clear that early and late growth are, in part, regulated by different underlying physiological mechanisms (Cheverud, 2005).

For the most part, QTLs influencing early growth were manifested by larger body weights in heterozygotes, or those mice with a genetic contribution from CAST, while QTLs affecting later growth almost always led to higher body weight when in the homozygous M16i genotype. Larger body weights for heterozygotes compared with homozygous M16 mice may represent a fitness advantage in that larger mice would have a higher survival rate than smaller mice during preweaning growth. The larger body weights of M16i-based alleles for later growth stages are not surprising. The basis for selection in the M16i line was for weight gain during the period of major postnatal growth from 3 to 6 weeks of age, and a correlated response to this selection is that the mice are late-maturing (Eisen, 1986). Therefore, it would be expected that loci influencing growth rates from 3 to 6 weeks as well as at later stages would be positive for M16i homozygous mice. This influence was the case for most growth rate QTLs, with a clear exception on chromosome 1, where the heterozygous genotype led to faster growth rate between 3 and 6 weeks of age, and the advantage for the M16i homozygous genotype was not manifested until mid-to late-life. The advantage for heterozygotes and/or CAST-based alleles at early growth periods (mainly preweaning) may be due to two interrelated explanations. First, CAST mice originated as a natural wild population and have probably had selective pressure placed on very early growth rate due to increased prenatal and neonatal competition and death. Furthermore, overdominance is likely to be of greater importance for

https://doi.org/10.1017/S0016672306007944 Published online by Cambridge University Press

Table 6. *Interval mapping of organ weights: locations (cM), LOD scores and confidence intervals (CI) of QTLs*

		Location		LOD[b]		CI[c]	
Trait[a]	Chromosome	Unadjusted[d]	Adjusted[e]	Unadjusted	Adjusted	Unadjusted	Adjusted
LIV	2	64		17·61		59–69	
	11	25		6·49		14–53	
SPL	4	49	44	6·51	5·35	24–67	23–64
	9	28	30	7·87	8·37	17–40	18–40
	2		73		3·97		65–77
	10		29		3·54		20–40
KID	1	71	76	6·89	7·09	53–87	60–90
	18	73	73	6·95	5·10	61–73	60–73
	2		86		8·49		66–100
	3		65		3·54		47–75

[a] LIV, SPL and KID represent weights of heart, spleen and kidney, respectively.
[b] The LOD 3·3 criterion is used for significance.
[c] cM location where the LOD score is one less than the peak.
[d] No adjustment for body weight at 12 weeks of age.
[e] Adjustment for body weight at 12 weeks of age.

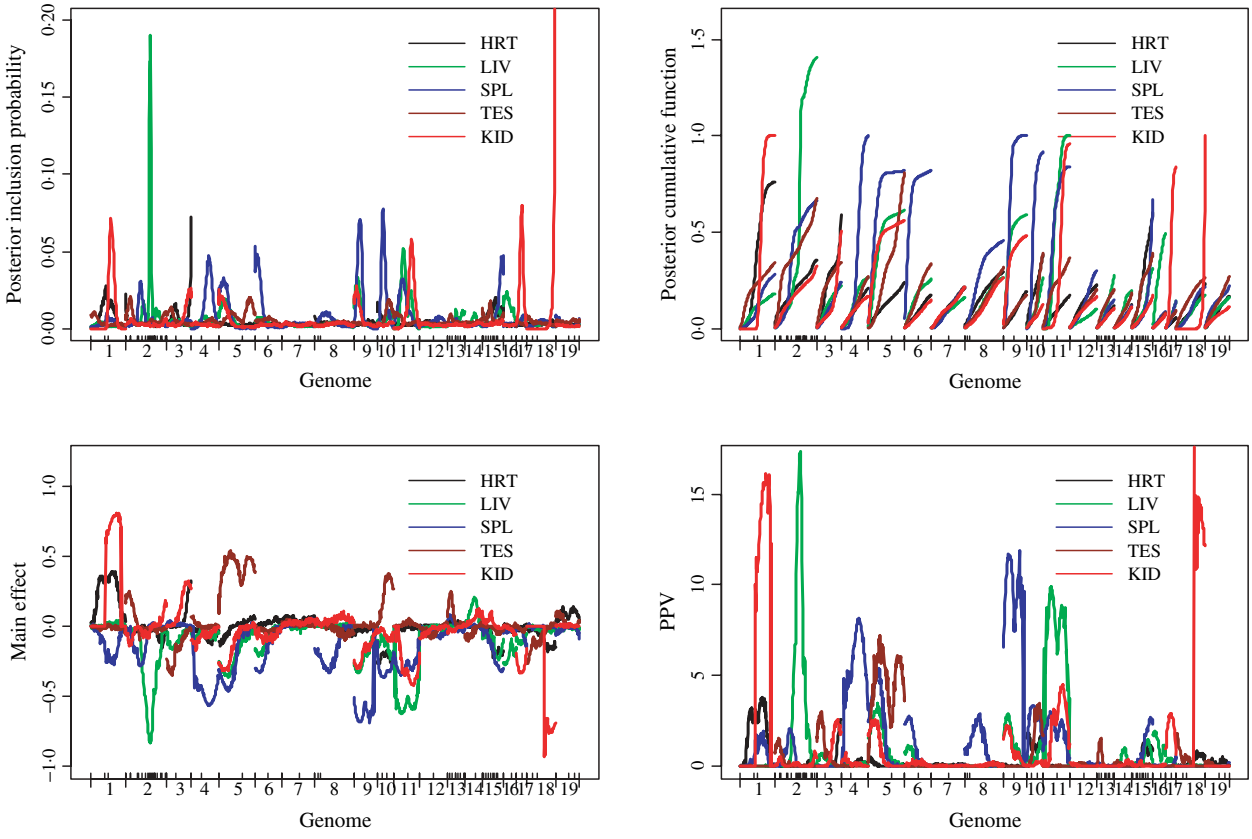

Fig. 4. Genome-wide epistatic analysis of organ weights under model excluding adjustment for body weight at 12 weeks: profiles of posterior inclusion probability, cumulative probability function, posterior means of main effect and proportion of phenotypic variance explained by main effect (PPV %). On the *x*-axis, outer tick marks represent chromosomes and inner tick marks represent markers. HRT, LIV, SPL, TES and KID represent weights of heart, liver, spleen, testis and kidney, respectively.

traits influencing fitness (Lerner, 1954) and would thus have greater importance in early as opposed to later growth rates. Indeed, Cheverud *et al*. (1996) have shown that overdominance was most prevalent for QTLs affecting early growth rate in their specific cross between LG and SM lines of mice. While we cannot separate overdominance from an additive effect with an advantage to the CAST allele, our data are again

https://doi.org/10.1017/S0016672306007944 Published online by Cambridge University Press

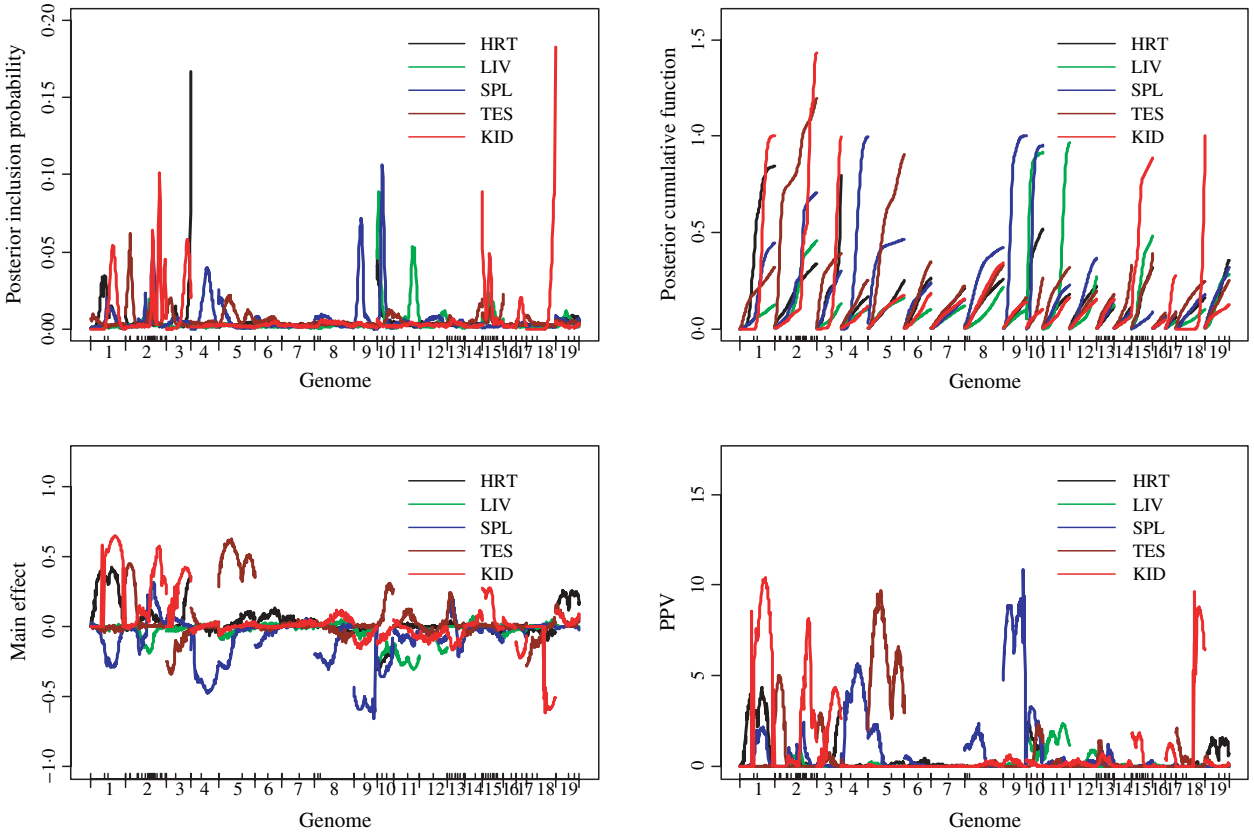

Fig. 5. Genome-wide epistatic analysis of organ weights under model including adjustment for body weight at 12 weeks: profiles of posterior inclusion probability, cumulative probability function, posterior means of main effect and proportion of phenotypic variance explained by main effect (PPV%). On the *x*-axis, outer tick marks represent chromosomes and inner tick marks represent markers. HRT, LIV, SPL, TES and KID represent weights of heart, liver, spleen, testis and kidney, respectively.

in general agreement with those of Cheverud *et al.* (1996).

The epistatic QTL effects on body weight in general agree with previous findings in mice (Cheverud *et al.*, 1996; Brockmann *et al.*, 2000, 2004; Ishikawa *et al.*, 2005). In a backcross between *M. m. castaneus* and C57BL/6J, Ishikawa *et al.* (2005) detected a higher degree of epistatic QTLs for juvenile growth compared with adult growth, which contrasts with the greater degree of epistasis for adult body weights than for juvenile weights found in the present study. The contrasting results may be associated with selection for post-weaning growth in M16 causing the build-up of epistatic complexes as ontogeny progresses.

(iii) *Adiposity QTLs*

The present study adds to the growing compilation of QTLs affecting adiposity in mice (e.g. Brockmann & Bevova, 2002; Rocha *et al.*, 2004*b*). Most QTLs affecting fatness have small additive effects, and several can be modified by diet, age and sex (Bünger & Hill, 2005). However, several studies have found significant epistatic interactions for fat deposits and related traits in mice and other mammalian species (Brockmann *et al.*, 2000, 2004; Cheverud *et al.*, 2001; Yi *et al.*, 2004*a*, *b*). Dong *et al.* (2003, 2005) reported two instances of epistasis between obesity-susceptibility loci in humans. Four pairs of interacting loci for non-insulin-dependent diabetes were detected in the Otsuka Long-Evans Tokushifa fatty rat (Yamada *et al.*, 2001).

The present data clearly indicate two types of adiposity genes with respect to body mass. One set of adiposity QTLs exhibit pleiotropy with body weight, which was expected based on positive genetic correlations and positive realized correlated responses previously reported (Eisen & Leatherwood, 1978*a*, *b*; Eisen, 1987). The other type of QTL for fatness is independent of body weight. Eisen *et al.* (1995) provided support for adiposity genes that are independent of body weight by successfully applying restricted selection to increase gonadal fat without altering body weight. Reducing fat content while holding body weight constant proved more elusive, possibly due to sensitivity of the index to changes in genetic parameters (Eisen *et al.*, 1995).

An interesting finding from this study was that epistatic interactions involving CAST alleles seemed to increase obesity (see Table 4). However, results

https://doi.org/10.1017/S0016672306007944 Published online by Cambridge University Press

Table 7. *Epistatic analysis of organ weights: cumulative posterior inclusion probability, posterior mean of epistatic effect and proportion of phenotypic variance explained by the epistasis* (*PPV%*)

Trait[a]	Chromosome pair	Posterior probability		Epistasis		PPV	
		Unadjusted[b]	Adjusted[c]	Unadjusted	Adjusted	Unadjusted	Adjusted
HRT	3 × 15	0·259	0·192	−0·689	−0·689	2·9	2·9
LIV	2 × 13	0·136		−0·500		1·5	
	4 × 16	0·140		−0·645		2·6	
	10 × 15		0·359		0·419		1·1
	11 × 19		0·215		0·472		1·3
SPL	4 × 5	0·439	0·109	0·771	0·607	3·7	2·3
	4 × 9	0·425	0·282	0·656	0·601	2·6	2·2
	5 × 9	0·197		0·622		2·4	
	6 × 11	0·291		0·651		2·6	
	11 × 12	0·131		−0·633		2·5	
	3 × 9		0·122		0·553		1·9
	12 × 19		0·167		−0·583		2·1
TES	1 × 15	0·128	0·106	0·882	0·836	4·8	4·3
	2 × 6	0·158	0·196	−0·789	−0·725	3·8	3·2
	11 × 15	0·121	0·109	0·866	0·807	4·6	4·1
	2 × 4	0·104		−0·837		4·3	
	2 × 5		0·103		0·446		1·2
	2 × 14		0·236		−0·878		4·8
	3 × 15		0·114		−0·877		4·8
KID	1 × 18	0·990	0·277	0·902	0·501	5·1	1·5
	1 × 11	0·394		0·632		2·4	

[a] HRT, LIV, SPL, TES and KID represent weights of heart, liver, spleen, testis and kidney, respectively.
[b] No adjustment for body weight at 12 weeks of age.
[c] Adjusted by covariance analysis for body weight at 12 weeks of age.

may again be confounded with dominance given that, in this backcross, all CAST alleles must appear in conjunction with an M16i allele. Evaluation of epistasis in an F_2 intercross would be more powerful than the current design, as it would enable comparison of the additive and dominance nature of epistatic interactions. We are currently performing such analyses using the cross described by Rocha *et al.* (2004*a*, *b*). Although the presence of CAST alleles on chromosome 2 appeared to outweigh the impact of the CAST alleles from other chromosomes on epistatic interactions, this probably reflects the very strong role of chromosome 2 on growth and obesity in this and other crosses involving the M16i line (Rocha *et al.*, 2004*a*, *b*). This region of the mouse genome appears to contain many genes involved in regulation of energy balance (Pomp *et al.*, 2004; Jerez-Timaure *et al.*, 2005).

Other consistencies of results can be found with the study of Rocha *et al.* (2004*a*, *b*), who crossed M16i and a second line selected for low 6 week body weight (L6). Our results reproduced the findings regarding coincidence of QTL locations affecting obesity traits. The QTLs for adiposity index located on chromosomes 2, 7, and 15 appeared to be in common. Also, the magnitude of concordance regarding QTLs for liver weight was very high. In contrast, it is not surprising that there were some discrepancies between the various studies employing the M16i line, due to different lines used for the cross (i.e. CAST/Ei versus L6), different adjustments of phenotypic data, and the lack of statistical detection of epistatic interactions in the study of Rocha *et al.* (2004*a*, *b*).

The QTL data here provide a possible explanation as to why selection for increased body weight in mice does not always lead to a positive correlated response in adiposity (e.g. Eisen *et al.*, 1978), even though the two traits are genetically positive correlated. If the QTL alleles that have a positive pleiotropic effect on adiposity and body weight are fixed or are at a low frequency such that genetic drift could cause loss of these alleles in early generations of selection, then directional selection for growth would lead to an absence of a correlated response in obesity.

Except for the interaction between chromosomes 1 and 18, which was shared for body weight and adiposity, different epistatic interactions were detected for different traits. Given that genetic correlations among these traits are high but far from unity (Eisen & Prasetyo, 1988), this evidence for partially independent pathways of interactive genetic control in addition to shared covariance is to be expected.

https://doi.org/10.1017/S0016672306007944 Published online by Cambridge University Press

(iv) *Organ QTLs*

Leamy *et al*. (2002) estimated QTLs for organ weights using these data and an interval mapping analysis (Haley & Knott, 1992). Although they detected more significant QTLs, probably due to use of principal components of all organ weights as a 'new' phenotype, the chromosomal regions detected by the two analyses appear to be very similar, for example chromosomes 1, 2, 4, 9, 11 and 18. Although QTLs for liver weight on chromosomes 2 and 11 were highly associated with total body mass, all QTLs for heart and testes weights, and some QTLs for weights of kidney and spleen, were independent of body weight. Results were comparable to those reported by Brockmann *et al*. (2000).

(v) *Conclusions*

The primary objective of this work was to apply Bayesian analyses of multiple epistatic QTL models to data on body weight and body composition in mice. Although we have uncovered statistical evidence for epistatic interactions contributing to the control of body weight and fatness, comprehensive functional analyses in the relevant regions must be undertaken to determine the underlying loci and how they interact. Fine-mapping is being actively pursued with congenic lines (Jerez-Timaure *et al*., 2005), but this targets QTLs with large main effects and not necessarily those with strong involvement on epistasis. The approach of integrating large-scale transcriptional phenotypes with QTL mapping (Schadt *et al*., 2003; Pomp *et al*., 2004) may be very powerful in discovering the genes involved in epistatic interactions.

For all analyses, QTLs with strong main effects on the phenotypes were identified on the same chromosomes no matter which method was applied. However, additional putative QTLs with relatively small influences on phenotypic variation were discovered only when assessing main effects and epistatic effects simultaneously, indicating that genes of small effect may only be detectable in models accommodating epistasis. The results of this study have thus not only added novel QTLs to the map of obesity predisposition in the mouse, but have provided some insights into potential interactions among genes that contribute to regulation of body weight and fatness. When comparing these results with other initial evaluations in other genetic crosses, different patterns of epistatic interactions emerge, suggesting the possibility of yet higher order interactions, as may be expected given the complex nature of the biochemical pathways regulating these traits. Given the important role that gene–gene interactions may play in regulating complex traits, it is clear that statistical models incorporating analysis of epistasis should be a focus of attention in future QTL analyses.

This research was supported in part by National Institutes of Health Grants GM069430, ES09912, DK056366 and DK056336.

References

Allan, M. F., Eisen, E. J. & Pomp, D. (2004). The M16 mouse: an outbred animal model of early onset obesity and diabesity. *Obesity Research* **12**, 1397–1407.

Allison, D. B., Pietrobelli, A., Faith, M. S., Fontaine, K. R., Gropp, E., *et al*. (2002). Genetic influences on obesity. In *Obesity: Mechanisms and Clinical Management* (ed. R. H. Eckel). New York: Lippincott Williams & Wilkins.

Atchley, W. R., Riska, B., Kohn, L., Plummet, A. & Rutledge, J. J. (1984). A quantitative genetic analysis of brain and body size associations, their origin and ontogeny: Data from mice. *Evolution* **38**, 1165–1179.

Atchley, W. R., Cowley, D. E. & Xu, S. (1997). Restricted index selection for altering developmental trajectories. *Genetics* **146**, 629–640.

Brockmann, G. A. & Bevova, M. R. (2002). Using mouse models to dissect the genetics of obesity. *Trends in Genetics* **18**, 367–376.

Brockmann, G. A., Kratzsch, J., Haley, C. S., Renne, U., Schwerin, M. & Karle, S. (2000). Single QTL effects, epistasis, and pleiotropy account for two-thirds of the phenotypic F2 variance of growth and obesity in DU6iXDBA/2 mice. *Genome Research* **10**, 1941–1957.

Brockmann, G. A., Karatayli, E., Haley, C. S., Renne, U., Rottmann, O. J. & Karle, S. (2004). QTLs for pre- and post-weaning body weight and body composition in selected mice. *Mammalian Genome* **15**, 593–609.

Bűnger, L. & Hill, W. G. (2005). Genetics of body composition and metabolic rate. In *The Mouse in Animal Genetics and Breeding Research* (ed. E. J. Eisen), pp. 131–160. London: Imperial College Press.

Carlborg, Ö. & Haley, C. S. (2004). Epistasis: too often neglected in complex trait studies? *Nature Reviews Genetics* **5**, 618–625.

Carlborg, Ö., Andersson, L. & Kinghorn, B. (2000). The use of a genetic algorithm for simultaneous mapping of multiple interacting quantitative trait loci. *Genetics* **155**, 2003–2010.

Chesler, E. J., Lu, L., Shou, S., Qu, Y., Gu, J., Wang, J., Hsu, H. C., Mountz, J. D., Baldwin, N. E., Langston, M. A., Threadgill, D. W., Mauley, K. F. & Williams, R. W. (2005). Complex trait analysis of gene expression uncovers polygenic and pleiotropic networks that modulate nervous system function. *Nature Genetics* **37**, 233–242.

Cheverud, J. M. (2005). Genetics of growth in the mouse. In *The Mouse in Animal Genetics and Breeding Research* (ed. E. J. Eisen), pp. 113–129. London: Imperial College Press.

Cheverud, J. M., Routman, E. J., Duarte, F. A. M., van Swindern, B., Cothran, K. & Perel, C. (1996). Quantitative trait loci for murine growth. *Genetics* **142**, 1305–1319.

Cheverud, J. M., Vaughn, T. T., Pletscher, L. S., Peripate, A. C., Adams, E. S., Erikson, C. F. & King-Ellison, K. J. (2001). Genetic architecture of adiposity in the cross of LG/J and SM/J inbred mice. *Mammalian Genome* **12**, 3–12.

Dong, C., Wang, S., Li, W. D., Li, D., Zhao, H. & Price, R. A. (2003). Interacting genetic loci on chromosomes 20 and 10 influence extreme human obesity. *American Journal of Human Genetics* **72**, 115–124.

Dong, C., Li, W.-D., Li, D. & Price, R. A. (2005). Interaction between obesity-susceptibility loci in chromosome regions 2p25–p24 and 13q13–q21. *European Journal of Human Genetics* **13**, 102–108.

Eisen, E. J. (1975). Population size and selection intensity effects on long-term selection response in mice. *Genetics* **79**, 305–323.

Eisen, E. J. (1986). Maturing patterns of organ weights in mice selected for rapid postweaning gain. *Theoretical and Applied Genetics* **73**, 148–157.

Eisen, E. J. (1987). Selection for components related to body composition in mice: correlated responses. *Theoretical and Applied Genetics* **75**, 177–188.

Eisen, E. J. & Leatherwood, J. M. (1978*a*). Adipose cellularity and body composition in polygenic obese mice as influenced by preweaning nutrition. *Journal of Nutrition* **108**, 1652–1662.

Eisen, E. J. & Leatherwood, J. M. (1978*b*). Effect of postweaning feed restriction on adipose cellularity and body composition in polygenic obese mice. *Journal of Nutrition* **108**, 1663–1672.

Eisen, E. J. & Prasetyo, H. (1988). Estimates of genetic parameters and predicted selection responses for growth, fat and lean traits in mice. *Journal of Animal Science* **66**, 1153–1165.

Eisen, E. J., Hayes, J. F., Allen, C. E., Bakker, H. & Nagai, J. (1978). Cellular characteristics of gonadal fat pads, livers and kidneys in two strains of mice selected for rapid growth. *Growth* **42**, 7–25.

Eisen, E. J., Benyon, L. S. & Douglas, J. A. (1995). Long-term restricted index selection designed to change fat content without changing body size. *Theoretical and Applied Genetics* **91**, 340–345.

Haley, C. S. & Knott, S. A. (1992). A simple regression method for mapping quantitative trait loci in line crosses using flanking markers. *Heredity* **69**, 315–324.

Hanrahan, J. P., Eisen, E. J. & Legates, J. E. (1973). Effects of population size and selection intensity on short-term response to selection for postweaning gain in mice. *Genetics* **73**, 513–530.

Hoeschele, I. (2001). Mapping quantitative trait loci in outbred pedigrees, In *Handbook of Statistical Genetics* (ed. D. J. Balding, M. Bishop & C. Cannings), pp. 599–644. New York: Wiley.

Ishikawa, A., Hatada, S., Nagamine, Y. & Namikawa, T. (2005). Further mapping of quantitative trait loci for postnatal growth in an intersubspecific backcross of wild *Mus musculus castaneus* and C57BL/6J mice. *Genetical Research* **85**, 127–137.

Jerez-Timaure, N. C., Eisen, E. J. & Pomp, D. (2005). Fine mapping of a QTL region with large effects on growth and fatness on mouse chromosome 2. *Physiological Genomics* **21**, 411–422.

Jiang, C. & Zeng, Z.-B. (1995). Multiple trait analysis of genetic mapping for quantitative trait loci. *Genetics* **140**, 1111–1127.

Lander, E. S. & Botstein, E. (1989). Mapping Mendelian factors underlying quantitative traits using RFLP maps. *Genetics* **121**, 185–199.

Lander, E. S. & Kruglyak, L. (1995). Genetics dissection of complex traits: guidelines for interpreting and reporting linkage results. *Nature Genetics* **11**, 241–247.

Leamy, L. J., Pomp, D., Eisen, E. J. & Cheverud, J. M. (2002). Pleiotropy of quantitative trait loci for organ weights and limb bone lengths in mice. *Physiological Genomics* **10**, 21–29.

Lerner, I. M. (1954). *Genetic Homeostasis*. New York: Wiley.

Lincoln, S., Daly, M. & Lander, E. S. (1992). Constructing genetic maps with MAPMAKER/EXP 3.0. Technical report. Cambridge, MA: Whitehead Institute.

Moore, J. H. (2005). A global view of epistasis. *Nature Genetics* **37**, 13–14.

Morris, K. H., Ishikawa, A. & Keightley, P. D. (1999). Quantitative trait loci for growth traits in C57BL/6J × DBA/2J mice. *Mammalian Genome* **10**, 225–228.

Plummer, M., Best, N., Cowles, K. & Vines, K. (2005). Output analysis and diagnostics for MCMC, R package version 0.10-3, URL http://cran.r-project.org/

Pomp, D. (1997). Genetic dissection of obesity in polygenic animal models. *Behavior Genetics* **27**, 285–306.

Pomp, D. (2005). Genomic dissection of complex trait predisposition. In *The Mouse in Animal Genetics and Breeding Research* (ed. E. J. Eisen), pp. 237–262. London: Imperial College Press.

Pomp, D., Allan, M. F. & Wesolowski, S. (2004). Quantitative genomics: Exploring the genetic architecture of complex trait predisposition. *Journal of Animal Science* **82**, E300–E312.

Rocha, J., Eisen, E. J., Van Vleck, D. L. & Pomp, D. (2004*a*). A large sample QTL study in mice. I. Growth. *Mammalian Genome* **15**, 83–99.

Rocha, J., Eisen, E. J., Van Vleck, D. L. & Pomp, D. (2004*b*). A large sample QTL study in mice. II. Body Composition. *Mammalian Genome* **15**, 100–115.

Rutledge, J. J., Robison, O. W., Eisen, E. J. & Legates, J. E. (1972). Dynamics of genetic and maternal effects in mice. *Journal of Animal Science* **35**, 1441–1444.

Schadt, E. E., Monks, S. A., Darke, T. A., Lusis, A. J., Che, N., *et al*. (2003). Genetics of gene expression surveyed in maize, mouse and man. *Nature Genetics* **422**, 297–302.

Segrè, D., DeLuna, A., Church, G. M. & Kiskony, R. (2005). Modular epistasis in yeast metabolism. *Nature Genetics* **37**, 77–83.

Sillanpää, M. J. & Arjas, E. (1998). Bayesian mapping of multiple quantitative trait loci from incomplete inbred line cross data. *Genetics* **148**, 1373–1388.

Vaughn, T. T., Pletscher, L. S., Peripato, A., King-Ellison, K., Adams, E., Erikson, C. & Cheverud, J. M. (1999). Mapping quantitative trait loci for murine growth: a closer look at genetic architecture. *Genetical Research* **74**, 313–322.

Warden, C. H., Yi, N. & Fisler, J. (2004). Epistasis among genes is a universal phenomenon in obesity: evidence from rodent models. *Nutrition* **20**, 74–77.

Wu, R., Chang-Xing Ma, C.-X., Hou, W., Corva, P. & Medrano, J. F. (2005). Functional mapping of quantitative trait loci that interact with the *hg* mutation to regulate growth trajectories in mice. *Genetics* **171**, 239–249.

Yamada, T., Miyake, T., Sugiura, K., Narita, A., Wei, K., Wei, S., Moralejo, D. H., Ogino, T., Gaillard, C., Sasaki, Y. & Matsumoto, K. (2001). Identification of epistatic interactions involved in non-insulin dependent diabetes mellitus in the Otsuka Long-Evans Tokushima fatty rat. *Experimental Animals* **50**, 115–123.

Yang, R. C. (2004). Epistasis of quantitative trait loci under different gene action models. *Genetics* **167**, 1493–1505.

Yi, N. & Xu, S. (2002). Mapping quantitative trait loci with epistatic effects. *Genetical Research* **79**, 185–198.

Yi, N., Xu, S. & Allison, D. B. (2003). Bayesian model choice and search strategies for mapping interacting quantitative trait loci. *Genetics* **165**, 867–883.

Yi, N., Diamont, A., Chiu, S., Kim, K., Allison, D. B., Fisler, J. S. & Warden, H. (2004*a*). Characterization of epistasis influencing complex spontaneous obesity in the B5B model. *Genetics* **167**, 399–409.

Yi, N., Chiu, S., Allison, D. B., Fisler, J. & Warden, C. H. (2004*b*). Epistatic interaction between two nonstructural loci on chromosomes 7 and 3 influences hepatic lipase activity in B5B mice. *Journal of Lipid Research* **45**, 2063–2070.

Yi, N., Yandell, B., Churchill, G., Allison, D., Eisen, E. J. & Pomp, D. (2005). Bayesian model selection for genome-wide QTL analysis. *Genetics* **170**, 1333–1344.

Zeng, Z.-B., Wang, T. & Zou, W. (2005). Modeling quantitative trait loci and interpretation of models. *Genetics* **169**, 1711–1725.

Zhang, Y. M. & Xu, S. (2005). A penalized maximum likelihood method for estimating epistatic effects of QTL. *Heredity* **95**, 96–104.